

Estimation of Electron Spectra Transitions of Free-Based Porphin and Mg-Porphin Using Various Quantum Chemical Approaches

Josef Šeda, Jaroslav V. Burda*, Veronika Brázdová, Vojtěch Kapsa

Department of Chemical Physics and Optics, Faculty of Mathematics and Physics, Charles University, Ke Karlovu 3, 121 16 Prague 2, Czech Republic

E-mail: Jaroslav Burda <burda@karlov.mff.cuni.cz>

* Author to whom correspondence should be addressed.

Received: 15 December 2003 / Accepted: 14 April 2004 / Published: 31 May 2004

Abstract: For optimized molecules of free-base porphin and magnesium-porphin (at Hartree-Fock level and 6-31G* basis set) excitation spectra were determined using several *ab initio* methods: CIS, RPA, CASSCF, and TDDFT. Obtained values were compared with semiempirical ZINDO method, other calculations found recently in literature and experimental data. It was demonstrated that for qualitatively correct spectra description the AO basis must include both the polarization and diffuse functions. The latter play an important role in formation of Rydberg MOs. Estimated energies of the spectra transitions using the CIS method remain relatively far from the measured values. RPA method can be already considered as a quantitatively accurate method when sufficiently large basis set is used. For CASSCF approach, it was shown that even the lowest energy transitions are insufficiently described in CAS formalism and much larger active space or inclusion of more inactive orbitals in correlation treatment would be necessary for obtaining sufficient accuracy. It can be stated that without sufficiently large correlation contributions, the determined spectra are not able to reach quantitative agreement with experimental data. From the methods treated in this study, only TDDFT can be considered as a useful tool for spectra prediction, at least for calculations of lower excited states. It is relatively fast and feasible for calculation of middle-size molecules. ZINDO approximation is also relatively successful for such large systems. Acceptable predictions of experimentally observed energy transitions in the range of Q and B bands were obtained. Until higher (UV) part of spectra is examined where the excitations to Rydberg orbital will happen, it can be considered as a good candidate for electron spectra calculations.

Keywords: porphin, magnesium-porphin, excitation spectra, CIS, RPA, CASSCF, TDDFT, ZINDO.

Introduction

Free-based porphin (FBP) and metalo-porphin molecules serve as test systems for practically all methods developed for electron spectra calculations.¹⁻¹⁴ Many of these studies were performed on qualitatively different basis sets and there leaves some uncertainty in the accuracy comparison of published results. Moreover usually not the same set of spectra transitions is compared. Authors often concentrate on the allowed (visible) part of spectra, which facilitates the calculations. The smaller number of spectra transitions allows to use a more extended basis sets or a larger active space and thus, such calculations are more accurate. One of the first calculations were done by Gouterman.^{15,16} He had used a four-orbital model within the Hückel method and by fitting parameters on experimental data he was able to reproduce basic spectral lines of porphin molecule and many of its derivates. It is interesting that even spectra of metalo-porphines (Cu porphin and its derivatives) were determined in ref.¹⁵ Later, Gouterman and Zerner¹⁷ published extended Hückel calculations on Mn – Zn metalo -porphines. Here besides spectra calculations also some other aspects were discussed. The cornerstone in ab initio calculation of spectral properties represents work from Pople group¹ where the CI-Singles method was introduced with all modern features like the analytical first derivatives and the correlation treatment for excited states within MP2 corrections. In this work also porphin excitation energies were computed within STO-3G till 6-31+G basis sets. The other method - Symmetry adapted cluster (SAC-CI) was proposed and used for FBP by Nakatsuji et al.¹⁸ and later also for chlorine and other related molecules.¹⁹ They calculated and discussed the effect of extended basis sets on porphin spectra in study¹³, where also higher Rydberg states were included and agreement for first four spectra transitions is very impressive – RMS=0.37 . In these calculation not only single but also double-excitation operators were included. Two years later Similarity transformed equation of motion (STEOM-CC) study on excited states of FBP appeared by Nooijen.²⁰ With the DZ character of the basis set the resulting spectrum is of the same accuracy (RMS=0.46 but no polarization and diffuse functions). When the CCSD step is replaced by MBPT(2) approximation STEOM-PT spectrum can be obtained as a cheaper version but substantial blue-shift (usually more than 0.2eV) can be observed for all calculated lines. The deterioration can be expressed by RMS value of 0.87. The same method was used with extended basis sets in study³ and improved excitation energies were obtained (RMS=0.27). Very accurate multireference CI calculation for the lowest singlet and triplet states was performed by Yamamoto²¹ where especially the first two lines are in perfect accord (within 0.02 eV) with measured excitations and resulting RMS is 0.08. Multireference CASPT2 spectra calculations of porphin and Mg-porphin molecules were published by Roos and Merchant.^{5,11,22,23} These calculations show similar deviation from the experiment (RMS=0.46). However, these authors point for the first time on the discrepancy between the intensities from calculated and experimental results. Their results support the original spectra assignment, where the B and N lines from the Soret band belong to two consequent pairs of B_{2u} and B_{3u} lines, in contrary with assignment suggested in SAC-CI studies. Thanks to the better accuracy of modern computational

techniques, the original spectra assignment is respected in all recent publications. The improved virtual orbital technique was applied in combination with the CASCI approach in study of Potts et al.²⁴

Recently applications of time dependent density functional theory (TDDFT) methods to porphyrin spectra were published.²⁵ More accurate calculations with different functionals (Becke-exchange²⁶ + Perdew-correlation²⁷) were done in a study of van Gisbergen et al..^{14,28} Their results are in accord with above mentioned assignment of B and N lines from the Soret band.

MRCI study²⁹ of porphyrin spectra using RAS active space was published recently by Werner's group. An experimental absorption spectrum of the magnesium-porphyrin (PMg) in the gas phase was not published yet. Usually for the experimental spectra comparison serve measured derivatives of PMg – 1,3,5,7-tetramethyl-2,4,6,8-tetraethylporphyrin-Mg (EthioPMg)³⁰ and 9,10,11,12-tetraphenylporphyrin-Mg (TPPMg).³¹

We decided to perform a more systematic study, which will contain some comparison on various basis sets for some methods. The electron spectra given by semiempirical ZINDO approach were compared with several ab initio methods. The CI-Singles, Random Phase Approximation (RPA), TDDFT with several functional (Becke3LYP, BP86, and B3PW91), and multireference CAS methods were chosen for this purpose. Based on these results relatively small and already sufficiently flexible basis set was chosen for the other method used for the testing purposes.

In this work we have dealt with electron spectra of free-base porphyrin and Mg-porphyrin and compare various approaches and the influence of the basis sets on the quality of the obtained spectra transitions

Computational Methods.

In our study, the HF/6-31G(d) optimization of free-based porphyrin and Mg-porphyrin was performed using D_{2h} and D_{4h} point group, respectively. In the paper of Almlöf et al.³², Lamoen et al.³³ and Merchan⁵, there were mentioned warning remarks on optimization of these species since a failure occurred due to resonance structures using the HF method without imposing symmetry restrictions. Both species are drawn Figure 1 together with the coordinate axes orientation (used later for characterization of obtained spectra transitions).

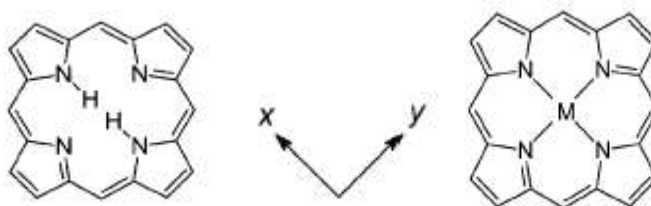


Figure 1: Free-base porphyrin and Mg-porphyrin together with standard orientation of the coordinate axes.

For the comparison of the individual spectra transitions several different basis sets were used in combination with various methods. The basis set dependence was examined within the configuration interaction with single-excitations (CIS) approach and the following AO bases were examined: Huzinaga minimal basis set MINI-3,³⁴ 3-21G,³⁵ 6-31G,³⁶ 6-31G**, 6-31+G, 6-31++G, 6-31+G* and 6-31++G**.^{37,38} The basis set dependence was verified on the electron spectra obtained with the random phase approximation (RPA).

Based on these calculations, sufficiently correct and still relatively small 6-31+G basis was chosen for substantially more demanding calculations e.g., the CASSCF method.

In multireference approaches, several active spaces were tested. In the case of FBP molecule, we started with the four-orbital model (signed as model A[4,4] with HOMO-1,...,LUMO+1 in $5b_{1u}$, $2a_u$, $4b_{2g}$, and $4b_{3g}$ irreducible representations) suggested by Gouterman.¹⁶ Second investigated active space was slightly enlarged by four virtual MOs $21a_g$, $18b_{2u}$, $18b_{3u}$, $15b_{1g}$ (model Ba[8,4]), which was further extended by two occupied ($4b_{1u}$ and $3b_{3g}$) and two unoccupied orbitals ($6b_{1u}$ and $3a_u$) in model Cb[10,8].

In previous CASSCF/CASPT2 studies^{11,22} concentrate only on visible spectral lines (B_{3u} and B_{2u} symmetry). They use basis sets without diffuse functions and deal only with π type orbitals in active space. The best published results are using 3- $6b_{1u}$, 2- $5b_{2g}$, 2- $5b_{3g}$ and 2- $3a_u$ active orbitals.

We chose two ways of the next active space extension. First we investigated active space with more Rydberg functions included, according to their eigenvalues (22 and $23a_g$, $19b_{2u}$, $19b_{3u}$, and $16b_{1g}$), model De[17,8]. Second way used was to extend the active space only with π type orbitals and it was found more important for excited states energy stabilization. Model Ec[13,10] extends the active space Cb[10,8] by occupied $3b_{2g}$ and virtual $6b_{1u}$ and $3a_u$ MOs, model F[16, 10] further by virtual orbitals $6b_{2g}$, $6b_{3g}$ and $4a_u$.

A synoptic representation of the active spaces used in CASSCF and CASPT2 is compiled in *Table 1*. A state-averaged wave function (density matrix) approach enables simultaneous calculation of several desired states (usually about 10) without substantial convergence difficulties.

	a_g	b_{2u}	b_{3u}	b_{1g}	b_{1u}	b_{3g}	b_{2g}	a_u
A					2	0	0	2
B	0	0	0	0	2	0	0	2
C	0	0	0	0	22	20	0	2
D	000	00	00	00	220	20	0	20
E	0	0	0	0	220	20	20	20
F	0	0	0	0	220	200	200	200
G	0	0	0	0	20	00	0	20
B'	0	0	0	0	20	0	0	2
C'	0	0	0	0	220	20	20	2

0 labels virtual orbital considered in given irrep.,
2 labels inclusion of occupied MO in given irrep.

Table 1. Active spaces used for spectra calculation at CASSCF and CASPT2 levels. FBP models are shown in the upper part, PMg model are signed with apostrophe.

However, some additional inaccuracy is brought in the determination of individual states. Therefore, state-specific calculations were also performed in chosen models of active spaces. In these cases, wave function optimization of some excited states converged only with great difficulties or not at all. Moreover, despite the apparent differences, the basic trends in shifts of spectra transitions with various active spaces were conserved for both types of computations. CASPT2 was performed only in the case of FBP molecule in smaller active space – labeled as model G. Additional 6 electrons were correlated in PT2 treatment. Larger amount of electrons made the job unfeasible with our computational equipment. In the case PMg only two active spaces were considered over four-orbital model A[4,4] ($5b_{1u}$, $4b_{2g}$, $4b_{3g}$, and $2a_u$). Model B is based on extension of model A with virtual orbitals $23a_g$, $19b_{2u}$, $19b_{3u}$, $15b_{1g}$, and $7b_{1u}$ to [9,4] active space and the largest model C contained additional occupied $5b_{1u}$, $4b_{2g}$, and $4b_{3g}$ orbitals (cf. lower part of the *Table 1*).

TDDFT spectra calculations were performed using B3LYP, B3PW91 and BP86 functionals. Test calculations with the B3LYP functional and various basis sets (6-31+G*, 6-311+G*, 6-311++G**) gave only small difference in calculated spectra, so 6-31+G* basis set was chosen for the rest of calculations. Spectra calculated on previously optimized (HF/6-31G* level) and DFT/6-31+G* reoptimized structures were compared. Since the main goal of this study concerns the accuracy of the quantum chemical methods available for calculation of electron spectra of larger-molecular models of photosynthetic centers, the semiempirical method ZINDO was also included into our set of methods. Geometry optimizations, CIS, RPA, and ZINDO electron spectra were calculated with the Gaussian 98 program package, multiconfiguration tasks were run with the Molpro program.

Transition spectra computations

Geometry optimizations, CIS, RPA, and ZINDO electron spectra were calculated with the Gaussian 98 program package, multiconfiguration tasks were run with the Molpro program.

Free-base porphyrin : the molecule of FBP has 81 occupied MOs and the ground state has electron configuration of D_{2h} symmetry group: $20a_g^2 17b_{2u}^2 17b_{3u}^2 14b_{1g}^2 5b_{1u}^2 3b_{3g}^2 3b_{2g}^2 2a_u^2$. The ordering of the HOMO-3 till HOMO orbitals at Hartree-Fock level is $4b_{1u}$, $3b_{3g}$, $5b_{1u}$, and $2a_u$ in all the examined bases with the Mini-3 exception where inverted order of HOMO and HOMO-1 appeared. However, the same order is predicted for all functionals in the DFT treatment. This difference in eigenvalues is less than 0.01 a.u. (similarly to the other basis) but with opposite sign. This exchange has no influence on the energy order of spectral transitions since it is inverted, too. In the virtual space, the agreement within several lowest orbitals is substantially worse as one could expect. LUMO and LUMO+1 belong to B_{2g} and B_{3g} irreps. However, the next order depends on the presence of polarization functions (even in larger basis sets with diffuse functions). In the sets where higher angular momentum functions are present, $4b_{3g}$ MO lies lower. LUMO+2 and higher orbitals already reflect a presence of the diffuse functions, i.e. they have Rydberg character if sufficiently flexible basis set is used.

First, the influence of various basis sets on CIS electron spectra was examined. All spectral energies are collected in *Table 2*. The smallest basis sets without any polarization and diffusion functions exhibit remarkable blue shifts of all the calculated lines. In more extended bases, two different trends are visible. Namely, the first two lines ($1B_{3u}$ and $1B_{2u}$) are more substantially influenced by polarization functions than by diffuse ones. This is easy to understand, since these lines originate from HOMO and HOMO-1 transitions to LUMO and LUMO+1. Their character is correctly described even in smaller bases but polarization functions allow substantially higher flexibility necessary for better description, e.g. passing from 6-31G to 6-31G(d,p) improves $1B_{3u}$ by 0.07a.u. while $2B_{3u}$ by only 0.03 and for the basis set extent by diffuse function the corresponding changes are 0.01 and 0.09 a.u., respectively. In the higher states, excited electrons are not bound so tightly and thus diffuse functions start to play more important role. Interestingly, the invisible $1B_{1g}$ line (excitation from HOMO-2 to LUMO) is practically constant from the double-zeta character of the basis set. From *Table 2*, the comparison with experimental data is also available. It can be noticed that even in the largest basis sets the agreement is still very disappointing and poor convergence with increasing bases can be remarked. The possible explanation can be searched in the simplicity of the electron excitation since only single excitations are considered and as pointed by Roos et al.,³⁹ for higher states the doublet-excitation character exhibits a more important role. Moreover CIS suffers with the lack of the correlation energy. In the last column the RMS from five lowest experimental spectrum lines is calculated. This criterion clearly demonstrates that the predicted spectra are far from being correct.

Even for the most extended basis set the RMS remains above 2.6.

Metho d	Basis set	1B ₃	1B ₂	2B ₃	2B ₂	1B ₁	3B ₃		1B ₂	1B ₁	1B ₃	1B ₂	2B ₃	2B ₂	3B ₃	RMS	
		u	u	u	u	g	1A _g	u	1A _u	g	u	u	u	u	u		
CIS	Mini	2.7	3.1	4.9	5.6	5.1	6.3	6.1	6.2	6.1	5.9	0.0	0.0	1.1	3.5	3.0	3.88
		5	0	8	1	0	6	3	1	1	8	1	1	8	9	2	9
	3-21G	2.5	2.7	4.6	4.9	5.0	5.8	5.5	6.5	6.5	6.4	0.0	0.0	1.6	3.0	2.0	2.936
		7	3	6	6	1	5	9	5	1	7	1	1	8	5	0	
	6-31G	2.5	2.6	4.6	4.8	5.0	5.7	5.5		6.5	6.5	0.0	0.0	1.8	3.0	1.8	2.860
		4	8	5	8	2	8	2		7	5	1	2	1	1	2	
	3-21G**	2.5	2.6	4.6	4.9	5.0	5.7	5.5		6.7		0.0	0.0	1.6	2.9	1.9	2.833
		1	4	3	2	0	5	6		1		4	3	3	7	7	
	6-31G**	2.4	2.5	4.6	4.8	5.0	5.6	5.5		6.7		0.0	0.0	1.7	2.9	1.8	2.767
		7	9	2	5	1	8	0		3		4	3	6	3	0	
cc-pvdz	2.4	2.5	4.5	4.8	4.9	5.6	5.5				0.0	0.0	1.7	2.9	1.8	2.763	
	6	7	9	2	9	5	4				4	3	4	4	2		
6-31+G	2.5	2.6	4.5	4.7	5.0	5.6	5.4	5.4		5.5	0.0	0.0	2.0	3.0	1.5	2.687	
	3	6	9	6	0	7	4	4		9	1	2	2	1	9		
6-31++G	2.5	2.6	4.5	4.7	5.0	5.6	5.4	5.0	5.2	5.2	0.0	0.0	2.0	3.0	1.5	2.687	
	3	6	9	6	0	7	4	2	7	0	1	2	2	1	9		
6-31+G*	2.4	2.5	4.5	4.7	5.0	5.5	5.4	5.1	5.5	5.6	0.0	0.0	1.9	2.9	1.5	2.619	
	6	7	7	3	0	6	2	9	4	0	4	3	8	5	7		
6-31++G**	2.4	2.5	4.5	4.7	4.9	5.5	5.4	4.7	5.0	5.2	0.0	0.0	1.9	2.9	1.5	2.605	
	6	7	6	2	9	5	1	9	6	4	4	3	7	5	6		
RPA	Mini	2.1	2.5	4.4	4.7	4.9	6.1	5.6	6.1	6.0				1.1	1.8	1.0	2.756
		7	8	7	7	8	6	9	9	9		0	0	1	6	6	
	3-21G	1.9	2.1	4.1	4.2	4.9	5.6	5.2				0.0	0.0	1.2	1.5	0.6	2.041
		8	8	2	4	0	3	8				1	1	8	8	0	
	6-31+G	1.9	2.1	4.0	4.1	4.8		5.1	5.4	5.7	5.5	0.0	0.0	1.4	1.5	0.4	1.894
		3	0	4	0	9		9	4	4	8	1	1	0	8	8	
	6-31+G*	1.7	1.9	4.0	4.0	4.8	5.3	5.1	5.1	5.5	5.6	0.0	0.0	1.3	1.5	0.4	1.883
9		4	1	6	8	5	6	9	3	0	3	2	5	4	6		
6-31++G**	1.7	1.9	4.0	4.0			5.1	4.7	5.0	5.2	0.0	0.0	1.3	1.5	0.4	1.873	
	8	4	1	5			5	8	6	4	3	2	5	3	6		
6-311++G**	1.7	1.9	4.0	4.0	4.8	5.3	5.1	4.7	5.0		0.0	0.0	1.3	1.5	0.4	1.868	
	5	0	0	4	6	2	4	7	3		3	2	3	2	7		
ZINDO		1.7	2.0	3.5	3.6	3.8	3.6	4.2	4.5	4.4	4.4	0.0	0.0	2.0	2.5	1.1	0.772
		5	8	0	1	2	8	2	3	3	8	4	6	1	1	5	
BP86	631+G*	2.2	2.3	3.1	3.1	3.1	3.1	3.5	3.3	3.3	3.4	0.0	0.0	0.1	0.0	0.8	0.378
		4	7	3	7	0	5	8	8	8	2	0	0	8	7	0	
B3PW91	631+G* (opt)	2.1	2.2	2.9	2.9	2.8	2.9	3.4	3.3	3.3	3.3	0.0	0.0	0.1	0.0	0.7	0.611
		4	7	4	8	9	5	3	4	6	8	0	0	2	4	7	
B3LYP	631+G*	2.3	2.5	3.4	3.5	3.5	3.7	3.9	4.0	4.0	4.1	0.0	0.0	0.5	0.8	0.6	0.544
		5	0	4	7	8	6	4	9	8	6	0	0	9	8	6	
B3LYP	6311+G*	2.2	2.4	3.3	3.4	3.4	3.6	3.8	4.0	4.0	4.1	0.0	0.0	0.4	0.7	0.7	0.392
		9	5	4	8	3	1	3	7	6	4	0	0	8	4	5	
B3LYP	6311++G**	2.3	2.4	3.4	3.5	3.5	3.7	3.9	4.1	4.1	4.1	0.0	0.0	0.6	0.9	0.6	0.517
		4	9	3	5	7	5	3	2	0	9	0	0	0	0	6	
B3LYP	6311++G**	2.3	2.4	3.4	3.5	3.5	3.7	3.9	4.1	4.1	4.1	0.0	0.0	0.5	0.8	0.3	0.504
		3	8	2	5	6	4	2	2	0	9	0	0	9	8	3	
B3LYP	631+G* (opt)	2.3	2.4	3.4	3.5	3.5	3.7	3.9	4.1	4.0	4.1	0.0	0.0	0.5	0.8	0.6	0.491
		3	7	1	4	5	3	1	0	8	7	0	0	9	8	5	
B3LYP	631+G* (opt)	2.2	2.4	3.3	3.4	3.4	3.5	3.8	4.0	4.0	4.1	0.0	0.0	0.4	0.7	0.7	0.348
		7	2	1	5	0	8	0	7	6	3	0	0	8	5	4	
Experiment		1.9	2.4	3.3	3.3			3.6				0.0	0.0	1.1		<0.	
		8	2	3	3			5				1	6	5		1	

Table 2. Transition energies (eV) and oscillator strengths (a.u.) of the lowest excitations of FBP in dependence on the basis sets used. Experimental *data*⁴⁴ are included for comparison.

As to oscillator forces the situation is more satisfactory, at least a qualitative agreement was achieved already with smaller basis sets (cf. second part of *Table 2*). In these cases overlap between given MOs is the controlling factor and the orbital shape is not so sensitive to completeness of the basis set as the orbital energies.

The second method chosen for the confirmation of the basis set dependence was RPA. In this method triple-zeta quality basis sets were included, too. Obtained spectra transitions are summarized in the middle part of *Table 2*. RPA even with the simplest basis set gives comparable results as CIS method with the best double zeta basis. Nevertheless, the lowest two spectral lines converge with increasing basis functions towards too low energies (in comparison with experiment). Similarly to discussion in CIS part, practically no influence of the diffuse functions is noticeable on these lines on the contrary to higher state transitions. Also, passing from the double-zeta to the triple-zeta basis set does not bring any substantial improvement for visible spectrum and only small changes are noticeable in invisible part. Also RPA spectra still show large blue shift (larger than 0.5 eV for all the lines except of the two lowest). The RMS criterion is improved but still cannot reach quantitative character – the best estimation stay above 1.8. Intensities of the obtained lines are in better agreement with experimental data than CIS approach, especially intensities of higher B_{3u} and B_{2u} transitions. Character of all the investigated spectra transitions at the RPA level is similar to CIS only weights of individual MO excitations are usually slightly different.

	IR	E(eV)	E(nm)	Force	fr -> to	w	fr -> to	w	
CIS	1 B1U	2.53	490.3	0.01	81 -> 83	0.50	80 -> 82	0.48	78 B_{3u} -0.349
	2 B2U	2.66	466.2	0.02	81 -> 82	0.52	80 -> 83	-0.46	79 B_{1g} -0.342
	3 B1U	4.59	269.9	2.02	80 -> 82	0.43	81 -> 83	-0.42	80 B_{3u} -0.245
	4 B2U	4.76	260.3	3.01	80 -> 83	0.51	81 -> 82	0.45	81 A_u -0.236
	5 B3G	5.00	247.9	0.00	79 -> 82	0.66			82 B_{2g} 0.005
	6 B1U	5.44	227.9	1.59	78 -> 82	0.58			83 B_{1g} 0.007
	7 AU	5.44	227.8	0.00	81 -> 85	0.59			84 B_{1u} 0.066
	8 B3U	5.59	221.9	0.01	80 -> 85	0.58			85 A_g 0.067
	9 AG	5.67	218.5	0.00	81 -> 91	0.51	79 -> 83	0.41	91 A_u 0.103
	10 B1G	5.69	218.1	0.00	81 -> 84	0.66			
RPA	1 B1U	1.93	641.1	0.01	81 -> 83	0.71	80 -> 82	0.68	
	2 B2U	2.10	590.1	0.01	81 -> 82	0.69	80 -> 83	0.63	
	3 B1U	4.04	306.7	1.40	80 -> 82	0.40	81 -> 83	0.37	
	4 B2U	4.10	302.2	1.58	80 -> 83	0.44	81 -> 82	0.35	
	5 B3G	4.89	253.4	0.00	79 -> 82	0.65			
	6 B1U	5.19	238.8	0.48	78 -> 82	0.62			
	7 AU	5.44	228.0	0.00	81 -> 85	0.59			
	8 B3U	5.58	222.2	0.01	80 -> 85	0.57			
	9 B1G	5.68	218.2	0.00	81 -> 84	0.66			
	10 B2G	5.74	216.2	0.00	81 -> 86	0.61			

Table 3 MO transitions and their weight factors in the case of CIS and RPA/6-31+G electron spectra.
*default basis set is 6-31+G

In *Table 3*, a comparison of individual excitation weights can be seen for the 6-31+G basis set and CIS and RPA methods. Visible differences are only in the highest two states. RPA has omitted the 9th CIS state. Nevertheless, reliability of a such high-state determination is at least questionable. Some of the most important MO's (HF/6-31+G), which are involved in the excitation process, are drawn in *Figure 2*. Unfortunately according to RMS, both CIS and RPA predicted spectra are not better than spectrum computed by semiempirical ZINDO approach.

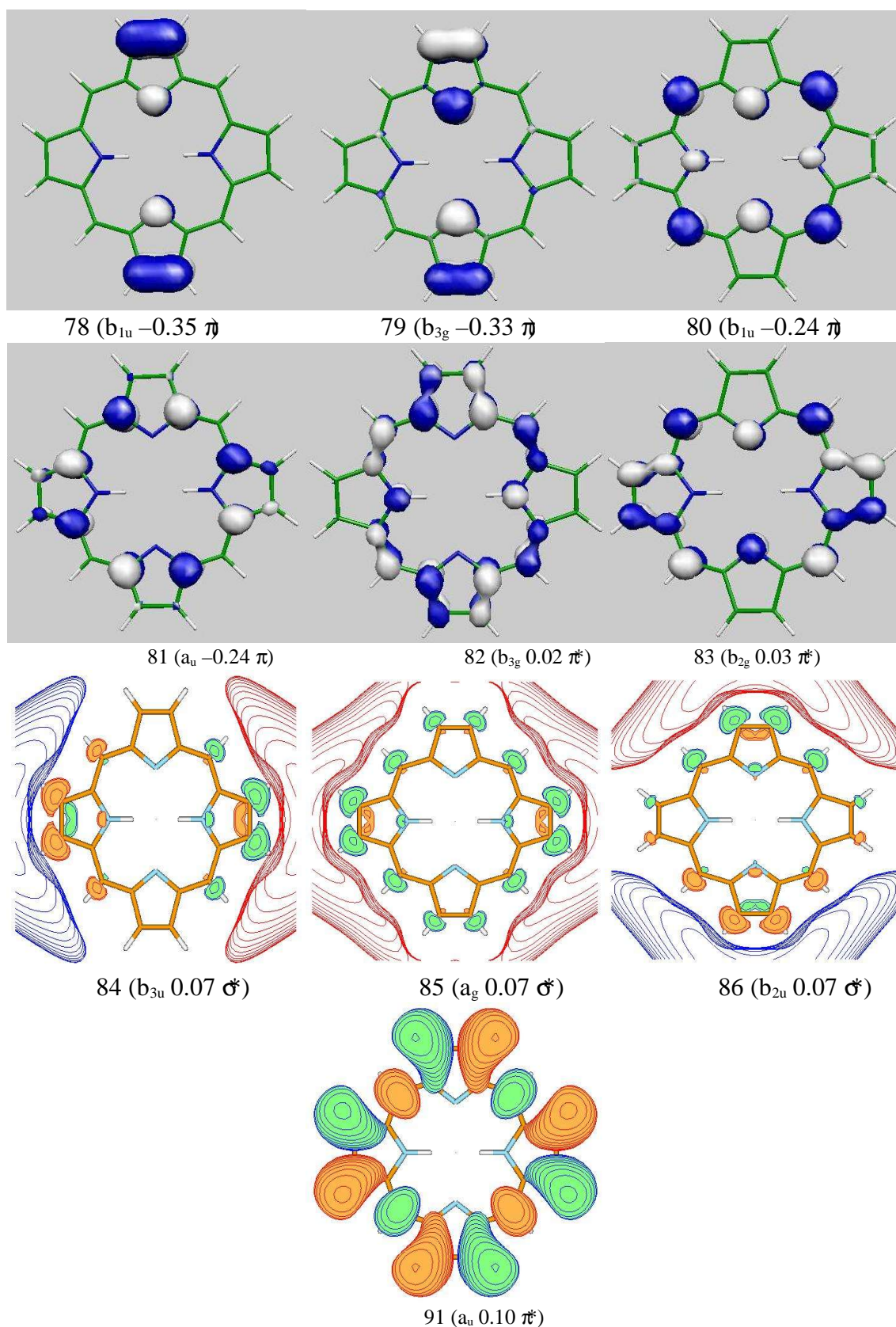


Figure 2. The most important MOs for interpretation of the lowest lines of electron spectra of FBP using CIS and RPA methods with 6-31+G basis set.

The last single-reference method is the TDDFT approach to spectra. On the contrary to RPA and CIS, it contains inherently the electron correlation. Only three different basis sets were used here, 6-31+G*, 6-311+G*, and 6-311++G**. Moreover the influence of the geometry optimization method (HF and DFT) on calculated spectra is evaluated within the DFT framework. Obtained spectra transitions are summarized in the end of Table 2. With exception of the BP86 functional, spectra calculated on the DFT optimized structure are closer to the experimental one than on HF geometry. Also, a very promising conclusion is that TDDFT spectra represent a substantial improvement approaching to the quantitative agreement with the experimental spectrum. All lines remain a few tenth spread around the measured transitions. The largest deviation occurs in the lowest line, similarly to RPA. However, a blue shift is noticeable in the TDDFT case. Also, RMS values are the best obtained from the calculations. Even for the HF geometry, the agreement with experimental lines is relatively good. In the contrary to lines energies their intensities are partially aggravated in comparison with other computational approaches. This holds especially for the 2B_{3g} and 2B_{2g} lines.

One of the best estimations of electron spectra should be expected from multireference methods based on the CASSCF approach. However, for systems with so many valence electrons, the active space must be drastically reduced in order to make these tasks feasible. The simplest model is based on 4-orbital approach published by Gouterman.¹⁶ However, all four predicted lines are more than 1.5 eV above the experimental results.

Model ^a	1B _{3u}	1B _{2u}	2B _{3u}	1B _{1g}	1A _g	2B _{1g}	2B _{2u}	1B _{3g}	1B _{1u}	1B _{2g}	2B _{2g}	2B _{1u}	2B _{3g}	3B _{3u}	2A _u	3B _{2u}	RMS
A	3.4	3.7	5.4					5.50									3.08
B^{av}	3.4	3.7	5.4	6.0	6.0		5.4	5.6	5.7	5.7	5.9	5.9	6.0	11.	6.1	11.	3.67
B^{so}	6	2	5	5	5	7.53	8	8	4	8	2	6	2	8	8	9	3
C	3.5	3.7	5.1	6.1	6.1		5.1	5.6	5.7	5.7							3.40
C/3-21++G**	3	7	3	6	6		6	6	0	4							5
D	3.3	3.6	4.8	4.9	5.4												3.51
E	2	2	8	0	1	6.08	5.37	5.70	5.53	5.76	5.72	5.95	5.79	5.98	5.96	6.26	6
F^{av}	3.3	3.6	4.8	4.9	5.3												3.924
F^{so}	3	2	7	1	7	6.11	5.37	5.26	5.19	5.35	5.35	5.56	5.44	6.02	5.64	6.23	3.08
G	2.8	3.5	4.9	4.4	5.2												3.08
G-PT2	8	9	2	7	7	5.64	5.36	5.67	5.41	5.62	5.80	6.03	5.74	5.81	5.89	6.36	8
H	2.6	3.7	5.0	4.9	4.9												3.67
I	6	5	8	5	6	5.13	5.27	5.49	5.27	5.58	5.46	5.77	5.57		5.71		3
J	2.3	3.9	4.8	4.4	4.5												3.40
K	7	3	6	3	4	5.08	5.12	5.61	5.38	5.57	5.81	6.00	5.80		5.82		5
L	2.3	3.9	4.9	4.7	4.5												3.51
M	9	6	8	4	9		5.19	5.86	5.44	5.87							6
N	3.0	3.3		5.3	5.1												3.41
O	4	7	5.05	1	0		5.06	5.71	5.96	5.78							3
P	2.4	3.2	4.5	4.5	4.5												2.83
Q	4	2	4	1	6		4.77	5.78	5.92	5.68							2
experiment	1.9	2.4	3.3				3.3							3.6			
	8	2	3				3							5			

^adefault basis set is 6-31+G

^{so} and grey lines signs the state-specific calculations, ^{av} means averaged-density calculations. CASPT2 contains electron correlation corrections of three MOs 4b_{1u}, 3b_{2g} a 3b_{3g} from inactive space.

Table 4. Dependence of the lowest transition energies (in eV) of the FBP molecule on the model of the active space and the basis set. For the comparison experimental values⁴⁴ are shown.

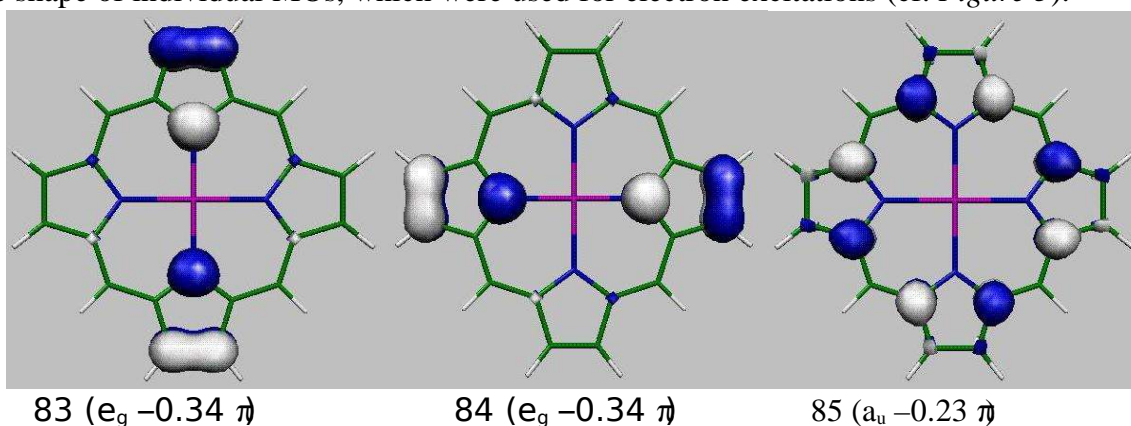
^{so} and grey lines signs the state-specific calculations, ^{av} means averaged-density calculations. CASPT2 contains electron correlation corrections of three MOs 4b_{1u}, 3b_{2g} a 3b_{3g} from inactive space.

From the *Table 4*, it can be seen that the extension to model B brings no substantial improvement either in the averaged density or in the single-state-specific approach. Some shifts towards the experimental energies are visible for most of the state transitions in the active space C. But even there, the minimal deviation is 1.2 eV. The influence of polarization functions is once more demonstrated for the CAS method in the active space C. It can be repeated that the main impact occurs in the spectra transitions in B_{1u} , B_{2g} , B_{3g} , and A_u irreducible representations where an up to 0.5 eV red-shift is obtained. In the further models D, E, and F the deviation (RMS in *Table 4*) is slowly decreasing, which clearly points to the fact that with sufficiently large active space the deviation will arrive under a desired threshold. Nevertheless, from chosen models, it is evident that the convergence is fairly slow with the increasing number of active orbitals. The importance of the inclusion of the correlation energy is demonstrated in the last two lines of *Table 4*. For a relatively small active space (G) with only four electrons, additional correlation corrections from next three lower occupied orbitals lead to relatively reasonable energies of most of the spectral lines (the RMS drops close to 2.8 from values larger than 3.0), achieving a comparable accuracy (in comparable CPU time) as CIS method with a substantially larger basis set. It can be remarked that the state-specific way of spectra calculation is more elaborate and leads to a worse RMS from the known experimental values. Moreover, many of the excited states converge with difficulties or does not converge at all as can be seen from missing numbers in *Table 4*.

It is obvious that correlation contributions play the key role for obtaining acceptable accuracy for the spectra prediction. When PT2 corrections are included or DFT method is used, despite single reference character, a pronounced improvement of spectra quality is achieved.

For larger molecular systems, even TDDFT can be too demanding. Therefore, semiempirical ZINDO method was regarded, too (see *Table 2*). The energetical order of valence MOs is in reasonable accord with the HF/6-31G** basis. The obtained spectrum is in a surprisingly good coincidence with experimental values. According to the RMS criterion, ZINDO predicts spectra only mildly worse than TDDFT methods and due to a very fortunate parameterization, which can also partially include the correlation effects, it gives even better results than all examined non-correlated calculations (including CASSCF). Transition intensities predicted by ZINDO are somewhat overestimated. Despite the very good agreement, one should be careful in the range of higher excited states since no Rydberg MOs are present in this semi-empirical approximation.

Mg-porphin : Analogous calculations, as for the FBP molecule, were performed also for PMg where two protons of the opposite pyrrole rings are replaced by the Mg^{2+} cation. This makes PMg even a more symmetric species (D_{4h} point group of symmetry). 172 electrons create the ground state configuration: $22a_g^2$, $18b_{2u}^2$, $18b_{3u}^2$, $14b_{1g}^2$, $6b_{1u}^2$, $3b_{2g}^2$, $3b_{3g}^2$, and $2a_u^2$. B_{2x} a B_{3x} irreps form a two-dimensional representation E_x (x means g or u). HF calculations gave the insight into the character and the shape of individual MOs, which were used for electron excitations (cf. *Figure 3*).



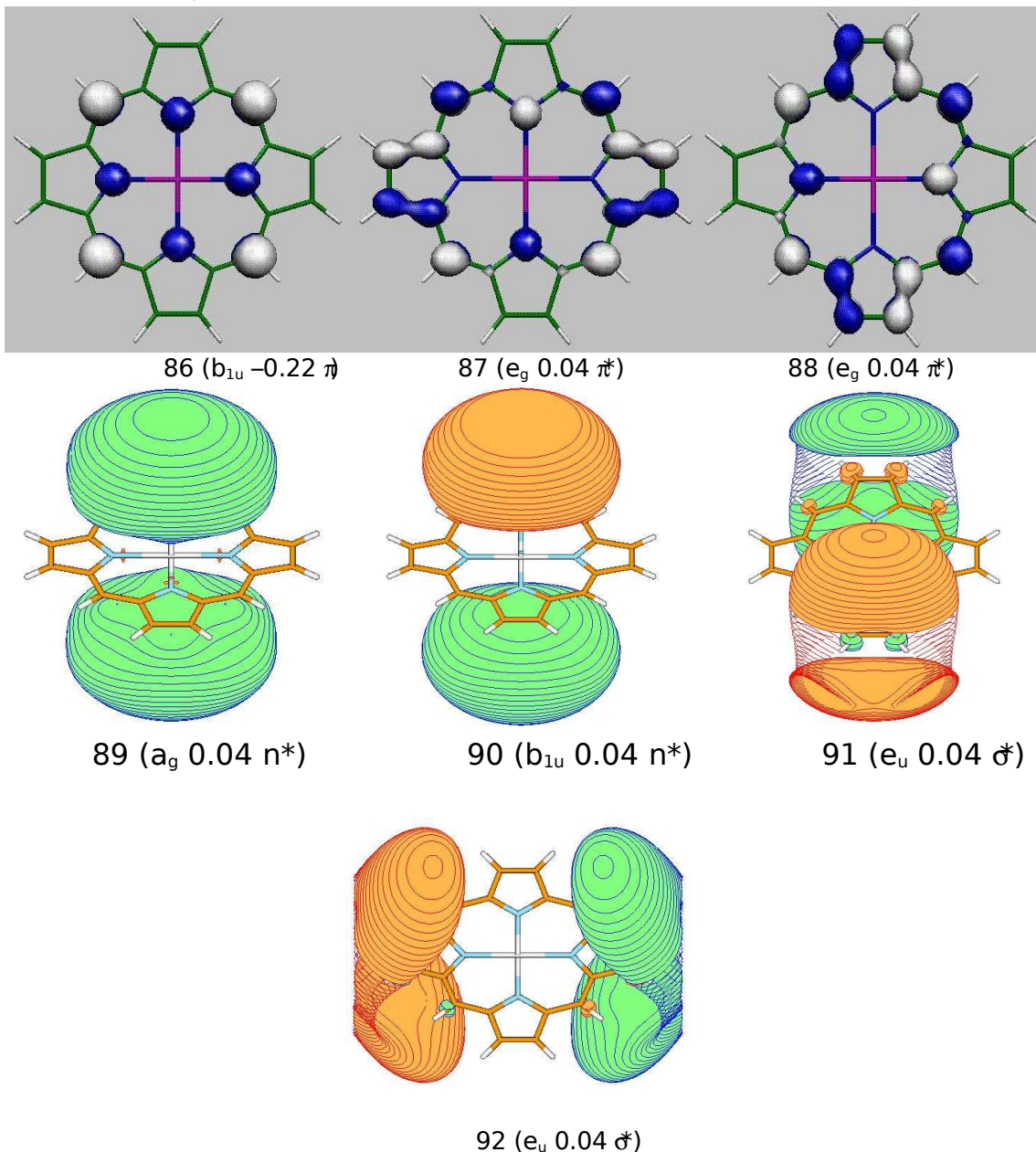


Figure 3. The MOs, which plays important role in the interpretation of the lowest state transitions in the PMg species using CIS and RPA/6-31+G.

These orbitals are very similar to MOs from FBP. The only visible exception present the first Rydberg orbitals, which belong to four diffuse AO 3s and 3p localized on the Mg^{2+} cation. Also, the symmetry restrictions put together b_{2g} and b_{3g} MOs, which are not degenerated in the FBP case and moreover the 78 (b_{1u}) MO separates one of their pair in FBP case.

Method	basis set	1E _u	2E _u	1B _{1g}	2B _{1g}	3E _u	1A _g	1E _g	1B _{1u}	1E _u	2E _u	3E _u
CIS	Mini	3.10	5.47	5.98	6.08	6.43	6.64			0.00	2.62	0.85
	3-21G	2.72	4.91	5.55	5.59	5.76	5.86			0.02	2.73	0.45
	6-31G	2.65	4.84	5.54	5.57	5.69	5.78			0.02	2.77	0.34
	3-21G**	2.69	4.85	5.54	5.58	5.71	5.84			0.01	2.67	0.35
	6-31G**	2.55	4.78	5.48	5.52	5.62	5.56			0.04	2.65	0.29
	cc-pvdz	2.54	4.76	4.58			5.17	4.92	4.91	0.05	2.66	
	6-31+G	2.61	4.73	4.86			5.10	5.08	4.85	0.02	2.87	
	6-31+G*	2.52	4.69	5.14	5.47	5.57	4.62	4.85	4.87	0.04	2.78	0.23
	6-31++G**	2.52	4.68			5.56	5.36	4.81		0.04	2.78	0.23
RPA	Mini	2.46	4.62	5.80	5.80	6.07	6.31			0.00	0.17	0.06
	3-21G	2.17	4.25	5.44	5.47	5.60	5.62			0.00	0.16	0.03
	6-31G	2.07	4.17	5.43	5.45	5.54	5.86			0.01	1.51	0.10
	6-31G**	1.91	4.12	5.38	5.40	5.47				0.03	1.42	0.09
	6-31+G	2.06	4.10	4.86			5.09	5.08	4.85	0.01	1.56	
	6-31+G*	1.89	4.06	5.14	5.36		4.62	4.85	4.86	0.03	1.49	
	6-31++G**	1.89	4.05			5.42			5.33	0.03	1.49	0.08
ZINDO		1.97	3.63	4.24	4.30	4.50	4.81	4.59		0.07	2.59	0.07
BP86	631+G*	2.32	3.34	3.40	3.43	3.41	3.45	3.86		0.00	0.22	0.54
	631+G* (opt)	2.22	3.15	3.20	3.23	3.26	3.26	3.83		0.00	0.06	0.57
B3PW91	631+G*	2.44	3.56	3.90	3.94	3.92	4.06	4.57		0.00	1.02	0.03
	631+G* (opt)	2.38	3.49	3.77	3.81	3.79	3.93	4.55		0.00	0.98	0.05
B3LYP	631+G*	2.43	3.55	3.89	3.93	3.91	4.05	4.60	4.57	0.00	1.03	0.03
	6311+G*	2.42	3.55	3.88	3.92	3.89	4.04	4.60	4.63	0.00	1.02	0.03
	631+G* (opt)	2.36	3.46	3.74	3.78	3.75	3.90	4.57	4.58	0.00	0.98	0.05
Experiment	Mg-Ethio	2.14	3.18	3.82								
	Mg-TPP	2.07	3.04	3.96								

Table 5 Transition energies (eV) and oscillator strengths (a.u.) of the lowest excitations of PMg in dependence on the basis sets used. For the comparison experimental data of Mg-ethioporphine and Mg-TPP (Mg-tetrapyrrole porphine) are included^{31,44}.

CIS estimations of the electron spectrum were similarly calculated in several chosen AO bases. Resulted transition energies are collected in the first part of Table 5 where the role of various types of functions is marked. As in the previous FBP case, the first two lines are more sensitive to the polarization functions. However, the extension with diffuse AOs leads to changes in the excited states ordering. This reflects a more pronounced importance of the Rydberg MOs than it was in FBP spectra. Slightly surprising is a behavior of the cc-pvdz basis set since even without augmented diffuse functions the same effect on MOs ordering as for the 6-31+G basis set is apparent. The analysis of transitions from the ground to excited states within the later basis sets reveals the role of the highest occupied and first virtual MOs in the excitation process. Also, the extent of the similarity with FBP molecule can be compared. The first two spectra transitions 1E_u originate from HOMO excitations to degenerated LUMO and LUMO+1; some portion of HOMO-1 to LUMO+1 and LUMO, respectively, similarly to analogous transitions in FBP. Then the 1A_u transition occurs, which is mainly realized by an excitation from HOMO (2a_u) to LUMO+2 - Rydberg's 89 orbital (23a_g MO which is represented by 3s AO of Mg). The second pair of spectra transitions 2E_u exhibits inverted

order of the weight factors in comparison with the $1E_u$ excitation – higher weights for HOMO-1 to degenerate $4e_g$ virtual orbitals LUMO and LUMO+1 and lower weights for HOMO to these $4e_g$ orbitals. The 6th line corresponds to the B_{1u} excitation from HOMO-1 to LUMO+2 closely followed (about 0.01eV) by B_{1g} . A quite unsatisfactory feature is evident from the last line in Table 5 with 6-31++G** basis where further reordering of the lower spectra transitions is predicted. So, the second set of diffusion functions located on hydrogen atoms play non-negligible role. The 6th and 7th state transitions are invisible E_g lines. Such a rearrangement is not confirmed by any other method and it can be considered as a CI-Singles break down

RPA method gives similar picture to CIS in the PMg case, too. In accord with the FBP case, better agreement for spectra transitions is achieved with experimental data. The improvement of excitation energies with increasing basis of AO is remarkable from second part of Table 5. Reasonable accuracy is achieved only for the first line (similarly to FBP). The second line remains blue-shifted about 1 eV and the third even 1.5 eV in comparison with measurements performed on modified PMg – Mg ethioporphine and Mg-tetrapyrrole porphine. The extension of AO basis set with diffuse functions gives rise to qualitatively new excited states, e.g. $1A_u$ or $1B_{1u}$. Also, diffuse functions on hydrogen atoms should be regarded for proper ordering of higher excitations (round $3E_u$ line). The transition intensities are in substantially better accord with observed spectra than in CIS case.

TDDFT spectra estimations for PMg led to the best agreement with measured data. BP86 gives again slightly worse results the other two functionals. Also, the importance of correct structure is shown, DFT-reoptimized geometry influences the obtained spectra more than the treatment of larger basis set (spectra for HF(opt)/6-311++G** versus DFT(opt)/6-31+G*). The comparable lines are determined within a few tenth of eV (0.2-0.4), which confirms high reliability of this approach at least for several lowest states. Several warnings appeared in literature for higher-lying states due to wrong density limits, which represents inherent DFT problem.⁴⁰⁻⁴²

	$1E_u$	$2E_u$	$3E_u$	$1A_g$	$2A_g$	$1B_{1g}$	$2B_{1g}$	$1B_{1u}$	$2B_{1u}$	$1E_g$	$2E_g$	$1A_u$	$2A_u$
4O	3.61	5.48											
A	3.61	5.49	8.11	5.26	6.08	4.94	6.07	5.00	5.87	5.08	5.44	4.68	6.21
A	3.52	5.11				5.04		4.96		5.12		4.75	
B	3.17	5.22	6.56	4.69	5.66	4.55	5.69	4.42	5.46	4.67	4.86	4.27	5.63
B	3.42	5.20		5.06		5.11		4.45		4.78		4.39	
Mg-Etio	2.14	3.18	3.82										
Mg-TPP	2.07	3.04	3.96										

Table 6 CASSCF/6-31+G calculations of electronic spectra PMg in the dependence on extension of the active space. Two different models – both averaged-densities and single-optimized states (grey lines) were treated. Experimental data of Mg-ethioporphine and Mg-TPP (Mg-tetrapyrrole porphine) are included for the comparison.^{31,44}

Based on experience with FBP CASSCF calculations, only three models of active spaces were treated in the PMg spectra predictions. These models come from 4 active electrons –model A and B' and more extended 10-electrons model C'. Active spaces used in the models are depicted in lower part of Table 1. The simplest 4-orbital model overshoots the excitation energies by more than 1.5 eV (cf. Table 6). On the contrary to FBP case, the other two models of active spaces improves the situation only marginally, leaving the smallest deviation about 1.3 eV.

The ZINDO method was used for comparison with demanding ab initio calculations for PMg, too. In analogy with the FBP molecule, agreement with experimental lines is very good. However, the already mentioned drawback insisted in deficiency of diffuse orbitals is more pronounced here. Position of the second and third transitions deviates from experiment more than 0.5 eV (cf. Table 5). This is somehow surprising since the most important 3s and 3p (relatively diffuse) AOs are present for the excited-states construction within ZINDO, too. The diffuse functions are more important in the inactive spectrum part where for instance line 1A_u or 1B_{1u} are completely missing. It is clear that Q and B bands, which are dominant in the experimental spectra of PMg derivatives³¹, are predicted with reasonable accuracy.

Comparison with recent computations

In Table 7 some recent calculations on both molecules are collected. Here can be easily seen that all correlated calculations are relatively close to the experimental data. For the FBP molecule, it is interesting to notice that the highly-correlated methods like CASPT2, STEOM or SAC-CI usually underestimate the 1st (Q_y) line by ~0.2 eV. This is also the case of RPA and ZINDO. SAC and CASPT2 methods usually underestimate by the same deviation also 2nd line. From this Table it is clear that double-zeta basis set character is sufficient for a reasonable agreement with the measured spectra. One interesting example where reasonable transition energies are presented at the CASSCF level can be demonstrated on 17th line CASSCF.⁴³ Here the individual CASCF energies of excited states were subtracted from the Hartree-Fock calculation of the ground state. Then very good agreement with experimental value was obtained.

	1B _{3u}	1B _{2u}	2B _{3u}	2B _{2u}	3B _{3u}	3B _{2u}	1B _{1g}	1B _{2g}	1B _{3g}	1A _g	1A _u	1B _{1u}
MRSDpCI ⁶	2.27	3.42	4.72	5.29								
MRSDspCI/DZ ⁺²¹	1.97	2.4	3.41	3.24								
CIS/6-31+G ¹	2.53	2.66	4.6	4.8								
CASPT2/DZ ²²	1.7	2.26	2.91	3.04								
	0.001	0.02	1.66	1.54								
CASPT2/DZ* ¹¹	1.63	2.11	3.08	3.12	3.42	3.53						
	0.004	0.002	0.91	0.70	0.46	0.83						
STEOM-CC/DZ ⁷	1.72	2.61	3.66	3.77	4.28	4.67	3.63	4.08	4.45	4.08	4.14	4.54
	-	0.02	1.03	1.42	0.71	0.44	-	-	-	-	-	0.004
STEOM-CC/DZ* ³	1.75	2.4	3.47	3.62	4.06	4.35	3.44	4.21	4.51	3.95	4.24	4.56
	4E-04	0.01	0.69	1.20	0.93	0.42	-	-	-	-	-	0.002
STEOM-CC/DZ ⁺³	1.7	2.59	3.63	3.74	4.22	4.63	3.56	4.05	4.41	4.04	4.09	4.48
	-	0.02	0.98	1.37	0.74	0.44	-	-	-	-	-	0.003
SAC-CI/DZ ¹⁸	1.75	2.23	3.56	3.75	4.24	4.52	3.55	4.05	4.37	4.25	4.18	4.51
	0.001	0.01	1.0	1.7	1.0	0.4	-	-	-	-	-	0.005
SAC-CI/DZ* ¹³	1.77	2.01	3.47	3.73	4.2	4.38	3.45	4.22	4.51	4.24	4.32	4.63
	0.003	0.01	0.77	1.62	1.32	0.34	-	-	-	-	-	0.003
SAC-CI/DZ ⁺¹³	1.7	2.19	3.43	3.62	4.08	4.36						
	0.002	0.01	1.10	1.87	1.09	0.44						
SAC-CI/4-31+G* ⁴⁵	1.81	2.1	3.47	3.69	4.23	4.4	3.46	4.35	4.29	4.29	4.15	4.18
	0.002	0.02	0.90	1.88	1.63	0.58	-	-	-	-	-	9E-04
CEO ⁴⁶	1.54	1.98	2.966	3.011	4.03	4.53						
	0.025	0.03	1.12	1.27	0.44	0.14						
TDDFT ¹⁴	2.16	2.29	3.01	2.98	3.41	3.47						
	0.01	0	0.04	0.13	0.90	0.73						
IVO-CASCI/3-21G ²⁴	2.83	3.5	5.07	5.11								
	1E-04	0.02	2.72	2.52								
MRMP ⁴⁷	1.63	2.55	3.1	3.25								
	0.003	0.01	1.61	1.53								
CASSCF ⁴³	2.07	2.38	3.41	3.95	4.13	4.07						
DFT/MRCI ⁸	1.94	2.38	3.07	3.17	3.79	3.7						
	7E-04	0	0.48	0.66	0.82	0.55						
Experiment ⁴⁴	1.98	2.42	3.33		3.65							
	0.01	0.06	1.15		0.1							

Table 7 Part a Spectra transitions published for FBP recently in literature

	1E _u	2E _u	3E _u	1B _{1g}	1B _{3g}	1A _g	1A _u	1B _{1u}
SAC-CI/DZ* ⁴⁸	2.01	3.63	4.15					
	0.00							
	2	1.99	0.07					
CEO ⁴⁶	1.79	3.09	4.36					3.93
	0.058	1.22	0.03					0.04
CASPT2/DZ* ²³	1.66	2.66	3.11					
	0.04	0.82	0.15					
MRMP ⁴⁷	2	3.07						
	0.011	1.561						
TDDFT ¹²	2.21	3.15	3.25	3.58				
	1E-04	0.06	0.58	0.39				
DFT/MRCI ⁸	2.16	3.25	3.63					
	0.00		0.03					
	2	1.27	4					
Exp. Mg-Ethio ³¹	2.14	3.18	3.82					
Exp. Mg-TPP ⁴⁴	2.07	3.04	3.96					

Table 7 Part b Spectra transitions published for PMg recently in literature

Calculations available for PMg are slightly less frequent but practically all the modern methods were already applied, too.

In the lower part of Table 7, it is demonstrated that all presented methods give very good results. CASPT2²³ stays slightly behind. In all these examples basis sets of double-zeta quality was utilized. Similarly to FBP molecule obtained results are of a sufficient accuracy. Moreover, since these molecules are relatively large further extension of basis set would cause computational difficulties.

Conclusions

- Electron spectrum of FBP molecule was calculated using CIS, RPA, CASSCF, TDDFT and ZINDO methods. It was demonstrated that for qualitatively correct spectra description the AO bases must be extended by both the polarization and the diffuse functions. The later play important role in the formation of Rydberg MO.
- The calculated transitions in B_{3u} a B_{2u} irreps. of the FBP molecule correspond to the experimental bands Qx, Qy, B, and N. The second two transitions 2B_{3u} a 2B_{2u} describe (in accordance with measurements, ref.⁴⁴) the band B.
- Estimated energies of the spectra transitions using the CIS method remain relatively far from the measured values. The main message of CIS part, arising from comparison with other methods, dwells in relatively slow convergence of individual spectrum line from measurements (RMS criterion) with increasing basis sets. Moreover accordance in the ordering of individual spectral transitions is not good even with the largest basis set used. This demonstrates the need to include both the correlation corrections and multiple (double) excitations in the CI expansion.
- RPA method can be already considered as a quantitatively accurate method when sufficiently large basis set is used. However, this condition is very difficult to fulfill for more extended molecular systems. RPA/6-31++G** slightly underestimated the transitions 1B_{3u} a 1B_{2u} for the other lines remain the energies still above the experimental data.

Using the same AO basis, the same MO are involved in transition to excited states of the given symmetry for both the RPA and CIS methods. On the contrary to CIS, the order of several lowest spectra transitions remains unchanged when AO basis sets are varied. This makes the RPA method more trustable.

- TDDFT is according to the obtained results and according to the other literature citations the most useful tools for determination of lower excitation states. Since it is a “single-determinant“ method, it is also relatively fast and feasible for calculation of middle-size molecules.
- The CASSCF approach cannot be used even for these model structures. It was shown that even the lowest energy transitions are insufficiently described in CAS formalism. Much larger active space or inclusion of more inactive orbitals in the correlation treatment would be necessary for obtaining a sufficient accuracy, then reasonable accord with the lowest experimental bands could be obtained.^{11,22} If not only irradiative (forbidden) part of spectra ought to be correctly described, it is important to extend the active space for some virtual MOs from irreps. A_g, B_{2u}, B_{3u}, and B_{1g}, too.
- ZINDO approximation is very successful for such a large systems. Acceptable predictions of experimentally observed energy transitions in the range of Q and B bands were obtained. It can be considered as a good candidate for electron spectra calculations until higher (UV) part of spectra is examined where the excitations to Rydberg orbitals will happen.

Acknowledgments

Authors thank to Prof. J. Hala from our department and Prof. F. Vacha from University of South Bohemian in České Budějovice for fruitful and helpful discussions. Financial support was obtained from grant agency of Charles University. This work was done due to generous CPU support of Computational Centers of Charles University in Prague, Prague's Technical University, Masaryk University in Brno, and West Bohemia University in Pilsen.

References

- (1) Foresman, J. B.; Head-Gordon, M.; Pople, J. A.; Frisch, M. J. *J. Phys. Chem.* **1992**, *96*, 135-149.
- (2) Almlof, J.; Fischer, T. H.; Gassman, P. G.; Ghosh, A.; Haser, M. *J. Phys. Chem.* **1993**, *97*, 10964-10970.
- (3) Gwaltney, S. R.; Bartlett, R. J. *J. Chem. Phys.* **1998**, *108*, 6790.
- (4) Hasegawa, J.; Ozeki, Y.; Ohkawa, K.; Nakatsuji, H. *J. Phys. Chem.* **1998**, *102*, 1320-1326.
- (5) Merchan, M.; Orti, E.; Roos, B. *Chem. Phys. Lett.* **1994**, *221*, 136-144.
- (6) Nagashima, U.; Takada, T.; Ohno, K. *J. Chem. Phys.* **1986**, *85*, 4524-4529.
- (7) Nooijen, M.; Bartlett, R. J. *J. Chem. Phys.* **1997**, *107*, 6812-6830.
- (8) Parusel, A.; Grime, S. J. *Porphy. Phthalocyanines* **2001**, *5*, 225-232.
- (9) Parusel, A. B. J.; Grimme, S. *J. Phys. Chem. B* **2000**, *104*, 5395-5398.
- (10) Parusel, A. B. J.; Wondimagegn, T.; Ghosh, A. *J. Am. Chem. Soc.* **2000**, *122*, 6371-6374.
- (11) Serrano-Andres, L.; Merchan, M.; Rubio, M.; Roos, B. O. *Chem. Phys. Letters* **1998**, *295*, 195-203.
- (12) Sundholm, D. *Chem. Phys. Lett.* **2000**, *317*, 392-399.
- (13) Tokita, Y.; Hasegawa, J.; Nakatsuji, H. *J. Phys. Chem. A* **1998**, *102*, 1843-1849.
- (14) van Gisbergen, S.; Rosa, A.; Ricciardi, G.; Baerends, E. *J. Chem. Phys.* **1999**, *111*, 2499-2506.
- (15) Gouterman, M. *J. Chem. Phys.* **1959**, *30*, 1139-1161.
- (16) Gouterman, M.; Wagniere, G. H. *J. Mol. Spec.* **1963**, *11*, 108-127.
- (17) Zerner, M.; M., G. *Theret. chim. Acta* **1966**, *4*, 44-63.
- (18) Nakatsuji, H.; Hasegawa, J.-y.; Hada, M. *J. Chem. Phys.* **1996**, *104*, 2321-2329.
- (19) Nakatsuji, H.; Hasegawa, J.; Ohkawa, K. *Chem. Phys. Lett.* **1998**, *296*, 499-504.
- (20) Nooijen, M.; Lotrich, V. *J. Chem. Phys.* **2000**, *113*, 494-507.
- (21) Yamamoto, Y.; Noro, T.; Ohno, K. *Int. J. Quantum. Chem.* **1992**, *42*, 1563-1575.
- (22) Merchan, M.; Orti, E.; Roos, B. *Chem. Phys. Lett.* **1994**, *226*, 27-36.
- (23) Rubio, M.; Roos, B.; Serrano-Andres, L.; Merchan, M. *J. Chem. Phys.* **1999**, *110*, 7202-7209.
- (24) Potts, D.; Taylor, C.; Chaudhuri, R.; Freed, K. *J. Chem. Phys.* **2001**, *114*, 2592-2600.
- (25) Stratmann, R.; Scuseria, G.; Frisch, M. J. *J. Chem. Phys.* **1998**, *109*, 8218-8224.
- (26) Becke, A. D. *Phys. Rev. A* **1988**, *38*, 3098.
- (27) Perdew, J. P. *Phys. Rev. B* **1986**, *33*, 8822.
- (28) Velde, G. T.; Bickelhaupt, F. M.; Baerends, E. J.; Guerra, C. F.; Van Gisbergen, S. J. A.; Snijders, J. G.; Ziegler, T. *J. Comp. Chem.* **2001**, *22*, 931-967.
- (29) Celani, P.; Werner, H. *J. Chem. Phys.* **2000**, *112*, 5546-5557.
- (30) Dorough, G. D.; Miller, J. R.; Huennekens, F. M. *J. Am. Chem. Soc.* **1951**, *73*, 4315.

- (31) Edwards, L.; Dolphin, D. H.; Gouterman, M. *J. Mol. Spectrosc.* **1970**, *35*, 90.
- (32) Almlof, J.; Taylor, P. *J. Chem. Phys.* **1987**, *86*, 4070-4077.
- (33) Lamoen, D.; Parrinello, M. *Chem. Phys. Lett.* **1996**, *248*, 309-315.
- (34) Andzelm, J.; Klobukowski, M.; Radzio-Andzelm, E.; Sakai, Y.; Tatewaki, H. *Gaussian Basis Sets for Molecular Calculations*; Elsevier: Amsterdam, 1984.
- (35) Pople, J. A.; Hehre, W. J. *J. Comput. Phys.* **1978**, *27*, 161-168.
- (36) Binkley, J. S.; Pople, J. A.; Hehre, W. J. *J. Am. Chem. Soc.* **1980**, *102*, 939-946.
- (37) Ditchfield, R.; Hehre, W. J.; Pople, J. A. **1971**, *54*, 724-728.
- (38) Hehre, W. J.; Ditchfield, R.; Pople, J. A. *J. Chem. Phys.* **1972**, *56*, 2257-2261.
- (39) Matos, J. M. O.; Roos, B. O.; Malmquist, P.-A. *J. Chem. Phys.* **1987**, *86*, 1458-1466.
- (40) Havlas, Z.; Michl, J. *J. Am. Chem. Soc.* **2004**, *submitted*.
- (41) Clark, A.; Davidson, E.; Zaleski, J. *CHEMICAL COMMUNICATIONS* **2003**, 2876-2877.
- (42) Hsu, C. *JOURNAL OF THE CHINESE CHEMICAL SOCIETY* **2003**, *50*, 745-756.
- (43) Yamamoto, S.; Tatewaki, H.; Kitao, O.; Diercksen, G. *Theor. Chem. Acc.* **2001**, *106*, 287-296.
- (44) Edwards, L.; Dolphin, D. H.; Gouterman, M.; Adler, A. D. *J. Mol. Spectrosc.* **1971**, *38*, 16.
- (45) Kitao, O.; Ushiyama, H.; Miura, N. *J. Chem. Phys.* **1999**, *110*, 2936-2946.
- (46) Tretiak, S.; Chernyak, V.; Mukamel, S. *Chem. Phys. Lett.* **1998**, *297*, 357-364.
- (47) Hashimoto, T.; Choe, E.; Nakano, H.; Hirao, K. *J. Phys. Chem. A* **1999**, *103*, 1894-1904.
- (48) Hasegawa, J.; Hada, M.; Nonoguchi, M.; Nakatsuji, H. *Chem. Phys. Lett.* **1996**, *250*, 159-164.